Available online at www.scholarsresearchlibrary.com

Scholars Research Library

Archives of Applied Science Research, 2013, 5 (2):138-144
(http://scholarsresearchlibrary.com/archive.html)

ISSN 0975-508X
CODEN (USA) AASRC9

Studies of PbS: Bi^{3+} nanocrystals synthesized by chemical bath

G. Hernández Téllez[a], K. Baxin Sánchez[a], S. Cruz Cruz[b], U. Peña Rosas[b], R. Gutiérrez Pérez[a], R. Palomino Merino[c], J. I. Contreras Rascon[b] and O. Portillo Moreno[a*]

[a]Lab. Síntesis de Complejos, Facultad de Ciencias Químicas, Benemérita Universidad Autónoma de Puebla. Puebla, Pué., México
[b]Dpto. Ing. Química, Universidad Politécnica de Tlax., Av. Universidad Politécnica No. 1, San Pedro Xalcaltzingo Tepeyanco, Tlax. México
[c]Facultad de Ciencias Fisicomatemáticas, Posgrado en Optoelectrónica, Benemérita Universidad Autónoma de Puebla. Puebla, Puebla, Pué., México

---

ABSTRACT

The growth of nanocrystallinePbS films by chemical bath (CB) onto glass at a temperature T = 40 ± 2°C is reported. The morphological changes of the layers were analyzed by Atomic Force Microscopy.X-ray diffraction spectra displayed peaks at 2θ = (26.00, 30.07, 43.10, 51.00, 53.48), indicating growth on the zinc blende face. The grain size determined by X-rays diffraction of the undoped samples was found ~32 nm, whereas with the doped sample was 25-15 nm.In optical absorption, forbidden band gap energy shift disclose a shift in the range 1.2-2.0 eV.

Keywords: Thin filmsQuantum confinement effect NanocrystalsPotential cell Coordination complex

---

INTRODUCTION

Lead sulfide (PbS) is one of the most important narrow-band compound semiconductor widely used as infrared sensor due to is 0.4 eV direct band gap (E_g). Following the pioneer theorical study of semiconductor nanocrystals (NCs) by Brus, tremendous efforts have been made to synthetize nanocrystalline with quantum size effects [1, 2]. PbS semiconductors NCs are of great interest for both fundamental research and technological applications because of the optical and electrical properties are likely to play a key role in the emerging new field of nanotechnology in applications ranging from optoelectronics to chemical sensing devices [3]. Due to this effect E_g of the material increases as the size of the particle decreases. This property makes it an excellent candidate for opto-electronic applications in many fields such as photography, IR detectors, solar absorbers, light emitting devices and solar cells [4, 5]. As the diameter of the semiconductor crystallite approaches the exciton Bohr diameter, its electronic properties start to change. The discrete structure of energy states leads to a discrete absorption spectrum of NCs. Thus, one observes an increase in the E_g of semiconductor with a decrease in the particle size [6]. Various NCs such as nanorods [7], nanowires, [8], star-shaped [9], and dendrites [10], chemical bath [11, 12] of PbS have been synthesized. The confinement effect appears as a shift in absorption spectra and the absorption to lower wavelengths, which is due to a change in the E_g and control over assembly through the preparation process. Thus, on this frame of reference, in the present work attempt has been made to prepare PbS and Bi^{3+}-doped nanostructured films by chemical bath (CB), in order to investigate structural and optical properties of undoped and doped-PbS films [13].

CHEMICAL REACTIONS AND EXPERIMENTAL PROCEDURE

The reactions for the growth of PbS films doped with Bi^{3+}weredetermined by employing the cell potential values in basic media as reported [14, 15]. The aforementioned steps allow the slow process at the substrate surface to take place predominantly over direct hydrolysis of thiourea in the bulk of the reaction bath as follow [12, 13, 15]

$$SC(NH_2)_2 + 3OH^- \Leftrightarrow CO_3^{2-} + S^{2-} + 7H^+ \quad (1)$$

$$[Pb(NH_3)_4]^{2+} + Pb + S^{2-} \Leftrightarrow PbS + Pb^{2+} + 4NH_3$$

$$\Delta G^o = + 335.48 \text{ KJ} \quad (2)$$

$$[Pb(NH_3)_4]^{2+} + H_2S + S^{2-} \Leftrightarrow PbS + 4NH_3 + S + 2H^+ + 2e$$

$$\Delta G^o = + 362.88 \text{ KJ} \quad (3)$$

$$HPbO^- + H_2O + [Pb(NH_3)_4]^{2+} + H_2S + S^{2-} \Leftrightarrow PbS + 4NH_3 + S + 2H^+ + Pb + OH^- + Pb^{2+}$$

$$\Delta G^o = +799.48 \text{ KJ} \quad (4)$$

Since$\Delta G^0 > 0$, and as such, the reaction is not a spontaneous process.

$$Bi^{3+} + 3e \Leftrightarrow Bi \Delta G^o = -89.16 \text{ KJ} \quad (6)$$

Preparation of polycrystalline PbS thin films on glass substrates was performed at a temperature of 40 ± 2°C for undoped and doped with $V_{[Bi3+]}$ grown by CB and pH = 11.0. The growth of PbS films with six different levels of doping $V_{[Bi2+]}$ were obtained by the addition *in situ*: 5, 10, 15, 20, 25, 30 mLs in the solutions for PbS growth $Pb(CH_3CO_3)_2$(0.01 M), KOH (0.5 M), NH_4NO_3(1.5 M), $SC(NH_2)_2$ (0.2 M) [13, 15]. The samples were labelled as PbS0 for the undoped sample and PbSBi5-PbSBi30 for the doped samples. The optimal concentration of the doping solution [$V_{[Bi3+]}$] $Bi(NO_3)_2$ (0.031 M) was determined after several trials, until films had attained good adherence. This solution is routinely added to the reaction mixture during the growth of the PbS films [13, 15].

The Atomic Force Microscopy (AFM) images of the films were obtained by a Nanoscoped E model contact mode AFM. The crystalline structure characterization was carried out by X-ray diffraction (XRD) patterns registered in a D8 Discoverdiffractometer, using the Cu K_α line. The optical absorption spectra, measured employing a Unicam 8700 Spectrometer, allow to calculate the forbidden band gap energy (E_g) by using the$(\alpha h\nu)^2$vs. $h\nu$ plot, where α is the optical absorption coefficient and $h\nu$ the photon energy.

RESULTS AND DISCUSSION

Atomic Force Microscope (AFM)

The surface images in an area of 10μm ×10μm of the PbS0-PbSBi thin films obtained by AFM are shown in Figures 1.Shown the 3D: (*a*) PbS0 indicate that growth of small grain distributed is rather different from each other indicated regular growth rate of the grains (*b*) PbSBi15 the grain density reduced indicating the smaller grain of PbS doped $V_{[Bi3+]}$ the size of the grain is noticed. The surface roughness is very small (6.5 nm) [13] (*c*) PbSBi30 shows that the small spherical nanograins of approximately 40-20 nm size were uniformly distributed over the smooth homogeneous background of crystalline phase

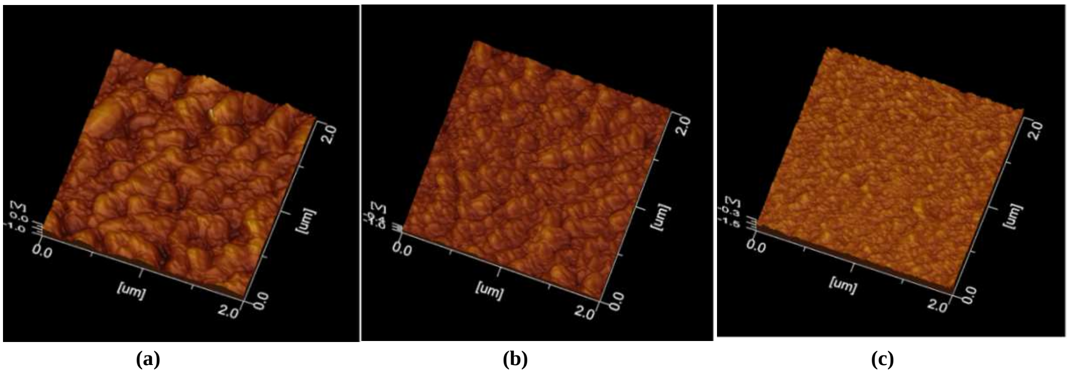

(a) (b) (c)

Figure 1. Images of Force Atomic Microscope PbS0-PbSBi thin films. (a) PbS0 (b) PbSBi15 (c) PbSBi30.

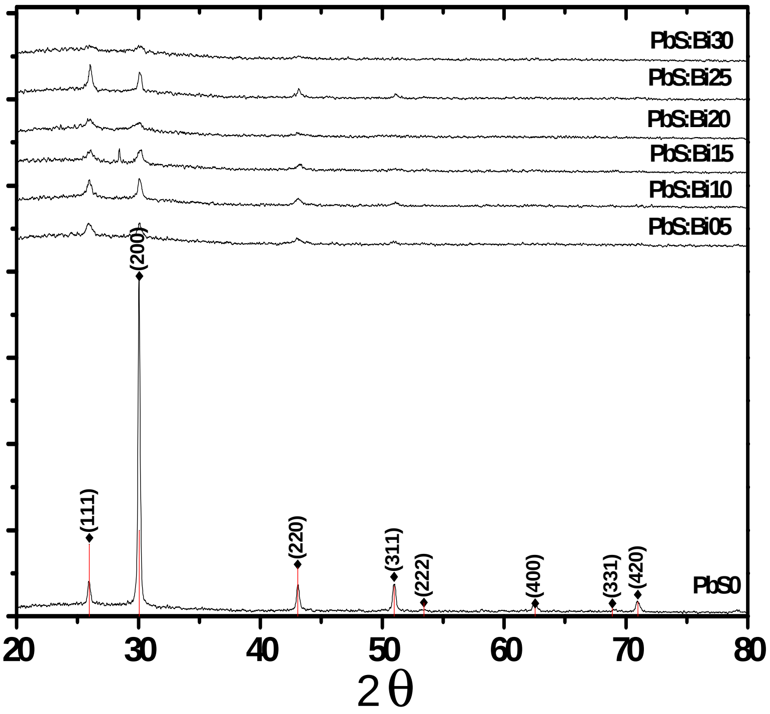

Figure 2. Diffractograms of X-ray (XRD) for doped and undoped PS0-PbSBi films.

X-Ray Diffraction (XRD)

Figure 2 shows diffractograms XRD of PS0-PbSBi films. Such X-ray spectra display peaks located at the following angular positions: 2θ = (26.00, 30.07, 43.10, 51.00, 53.48).All these diffraction peaks can be perfectly indexed to diffractograms of PS0-PbSBisamplesdisplaying the zincblende (ZB) crystallinephase according to reference patterns JCPDS 05-0592. However, the sample PbSBi15 show a peak 2θ = 28.605°, (211) defined XRD peak identical with the mineral bismuthinite (Bi_2S_3, PDF 17-0320). The XRD spectra for PbSBi0, indicating either the existence of a larger number of (111) planes or that the (111) planes have a lower number defects [16]. The low intensity peaks observed in the XRD patterns of the doped PbSBi20-PbSBi30 samples indicates that the films are coarsely fine crystallites or nanocrystalline [17]. The displayed pattern is due to an amorphous glass substrate and also possibly due to some amorphous phase present in the PbSBi crystallite size of films. There are two main possible causes for peak broadening. The first is an increase in heterogeneity of the films due to the occupation of Bi^{3+} into the host lattice. This phenomenon may be attributed to the doping effect [13, 18]. A second cause is a decrease in crystallite size, these effects are associated whit the nanocrystals doped-PbSBi with $V_{[Bi3+]}$ in the regime were the cluster mechanism is dominating (on the contrary to films grown via ion-ion mechanism, were the crystal size was larger), and consist of PbSBi nanocrystals embedded in an apparent matrix of PbS.

A possible explanation to this experimental fact can be given as follows: The ionic radii data are Pb^{+2} = 1.21 Å, S^{2-} = 1.84 Å and Bi^{3+} = 1.10 Å, and therefore, for a relative low concentration of Bi^{3+} ions a majority can be located in (*i*) Pb^{2+} vacancies sites, which otherwise would be empty (*ii*) in Pb^{2+} sites causing the appearance of Pb^{2+} interstitial, and (*iii*) in interstitial positions. It can be mentioned that the stable crystal structure of PbS, as a result, when Bi^{3+} occupies more and more sites of Pb^{2+} in the host lattice, internal strain would arise, and the crystal structure of PbSBi solid solution becomes unstable. In order to stabilize the crystal structure, the grain size is reduced to release the strain. Figure 3 shown average grain size (GS) vs. $V_{[Bi3+]}$ for PbS0-PbSBi samples corresponding to the (220) plane.

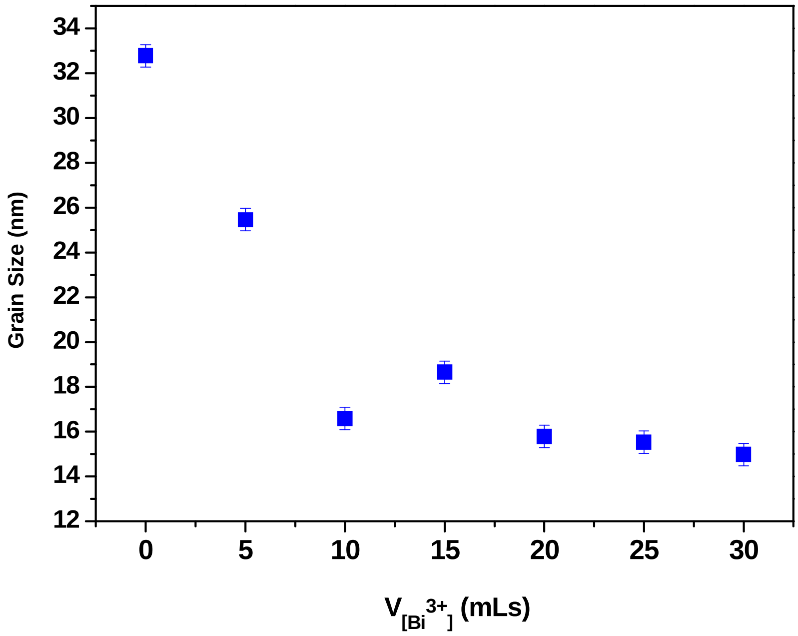

Figure 3. Average grain size (GS) vs. $V_{[Bi3+]}$ for PbS0-PbSBi samples corresponding to the (220) plane.

In this Figure can be observed that GS reduces, it can be seen for the PbS0, GS ~33 nm, and that the GS decreases for doped samples 25-15 nm range [13]. As the Bi^{3+} concentration is increased, the diffraction peaks become broader due to reduction in the grain size. At this level of $V_{[Bi3+]}$, the PbSBi can be considered a doped material [13, 15]. The effect of the GS decrease by the doping effect has been reported in films of PbS doped [19]. A decrease in the degree of order of crystallites is expected to lead to enhanced growth of stable nuclei at the initial stages of growth, followed by impaired grain growth, and hence resulting in smaller grains in the Bi.

ABSORPTION SPECTRA

The absorbance spectra vs. λ with various Bi content are depicted in Figure 4. In these spectra we appreciated that the absorbance decreases with the concentration of $V_{[Bi3+]}$. The intensity of the absorption increases steadily with the Bi content, and this is similar to most other reports on PbS nanoparticles [21]. The spectra of layers show an absorption onset of 600-700 nm with one salient shoulder at around 650 nm. A broad absorbance continuum can be seen rising from a long wavelength tail and peak ~500-650 nm for PbSBi10 and PbSBi15 layers. These exciton peaks were attributed to a $1S_e$-$1S_h$ transition [21]. Likewise, the intensity of the absorption increases steadily with the $V_{[Bi3+]}$, and this is similar the most other reports on PbS nanoparticles [22, 23]. The absorbance spectra of layers show an absorption onset of 500 nm with one salient shoulder around 600 nm. The excitonic absorption peak reported at ~600 nm is well-known that this peak is strongly related to surface change separation and polarization effects [23]. A broad peak located around ~655 nm (1.9 eV) appears after PbS nanocrystals produce. The energy transitions in both electron and hole levels of PbS nanocrystals was revealed in four major types, the S_e-S_h, S_e-P_h, P_e-S_h and P_e-P_h transitions [24].These exciton peaks were attributed to a $1S_e$-$1S_h$ transition. The intensity of the absorption increase steadily with the $V_{[Bi3+]}$, and this is similar the most other reports on PbS nanoparticles [22]. The excitonic absorption peak has been reported at ~600 nm [25]. This is a clear indication of the quantum confinement, since the average GS of the PbSBi nanocrystals is the exciton Bohr radius (18 nm). One the reasons for absence of exciton absorption peaks in the spectrum of PbS0 nanocrystals is that the nanocrystals are confined only in two directions and the third dimension is extended. This may washout the exciton absorption peaks in visible region [26].

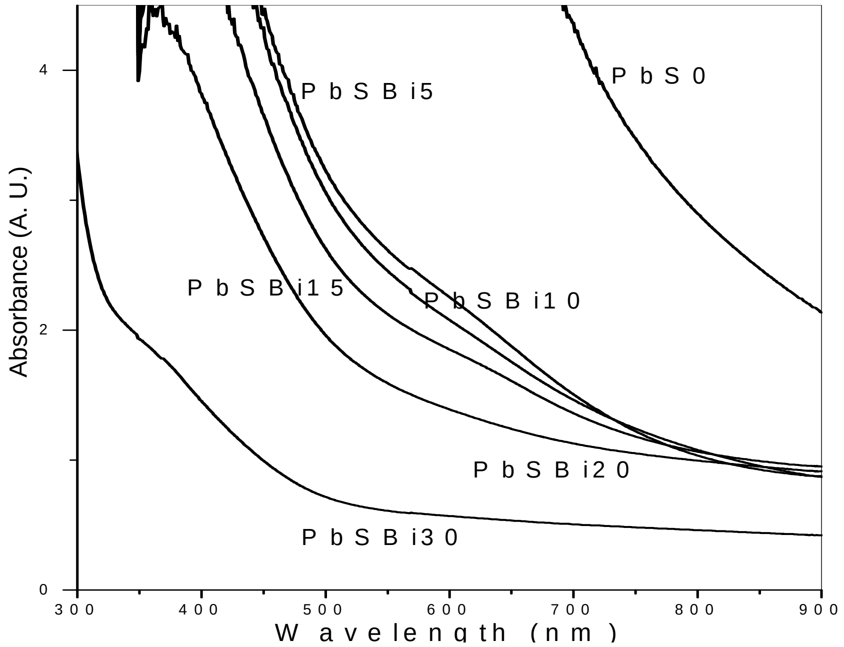

Figure 4. Absorbance spectra vs. λ with various Bi content.

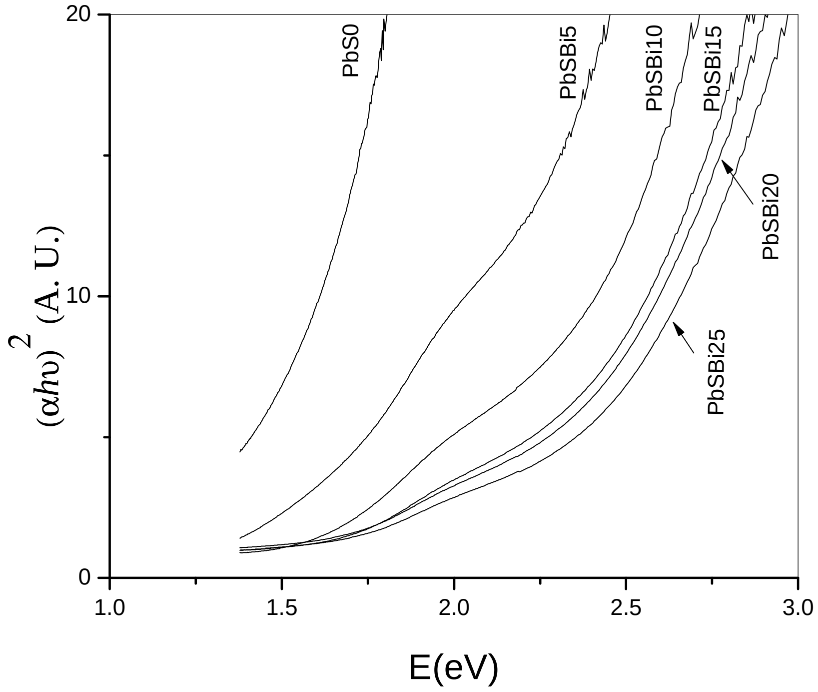

Figure 5. hvvs. $(\alpha hv)^2$plot for the nanoparticle PbS0- PbSBi film.

The direct E_g were obtained from linear portion of $(\alpha h\nu)^2$ vs. $h\nu$ plot, through the intersection of the straight line with the axis of the photon energy, an E_g value is obtained in a similar way to all samples[6]. In figure 5, theplot of $(\alpha h\nu)^2$ versus $h\nu$ for direct transition of PbS0-PbSBi layers is displayed.The confinement effect appears as a shift in edge of the absorption spectra and the absorption to lower wavelengths, possibly due to the decrease in GS and the decrease in number of defects. It is clearly seen from the optical spectrum an absorption edge shift toward a lower wavelength in doped films. This clearly indicates an increase in the E_g as a result of Bi-doping. Doping of PbS with Bi^{3+} is expected to alter the optical E_g between 0.41 eV (E_g of PbS) and resulting ternary PbSBi alloy [13, 19].Thus, the observed large modification of ternary PbSBi alloy and existence of strong quantum confinement in this system.

Previously, there were reports about very large Stokes shift in PbS quantum dots (QDs), which was attributed to the presence of localized surface states or trap states [27]. The excitonic peak at 1.73 eV is from ^1S_h to ^1S_e, which is also the optical E_g of this size PbS QDs. Though there has been debate over assignment of the excitonic transition at 1.42 eV, assign it as ^1P_h to ^1P_e. The excitonic at 1.66 eV, 1.86 eV, 2.157 eV, are due to higher energy transitions from ^1D_h to ^1D_e, ^2S_h to ^2S_e and ^2P_h to ^2P_e, respectively [27]. Emission band at 433 nm are usually related to the transition of electrons from the conduction band edge to holes, trapped at interstitials Pb^{2+} sites, the emission at about 433 nm presents a Stocks shift compared to the absorption band edge (226 nm) in the UV-vis absorption spectra [10]. The emission peak observed at 1.9 eV corresponds to the S_e-S_h transition which is a lowest energy exciton. The possibility of obtaining PbS optical E_g ranging from 0.41 eV by varying the crystalline diameter from 13 nm to 23 nm was reported [22].The Figure 6 showed $E_g$vs. $V_{[Bi3+]}$ plot for the nanoparticle PbS0- PbSBi film.

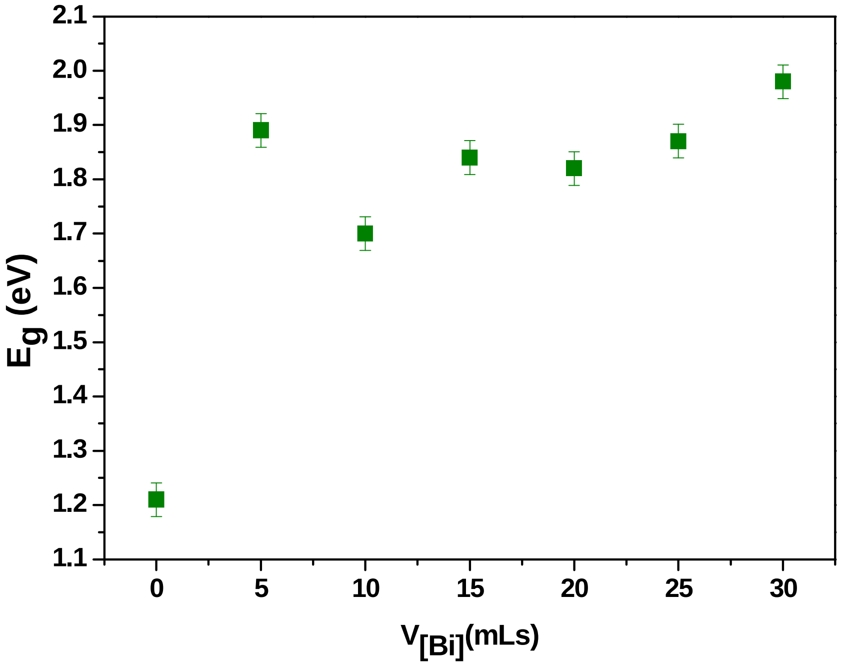

Figure 6.$E_g$vs.$V_{[Bi3+]}$ plot for the nanoparticle PbS0- PbSBi film.

CONCLUSION

In summary, we have found an efficient process to introduce Bi^{3+} ions into PbS lattice with, practically, no large damage to the lattice. XRD spectra show 2θ = (26.00, 30.07, 43.10, 51.00, 53. 48), which belong to the ZB phase. The grain size lies in the interval of 33-15 nm. Optical absorption spectra are quantified for the PbSBi film in which the redshift of E_g is associated with the decrease of the average GS. Forbidden band gap energy (E_g) shift disclose a shift in the range 1.2-2.0 eV.

REFERENCES

[1] L. E. J.Brus, *Chem. Phys*. **1984**,**80**, 4403-4409.
[2] Z.Peng, Y. Jiang, Y. Song, C. Wang, H. Zhang, *Chem. Mater*. **2008**,**20**, 3153-3162.

---

[3] R. Reisfeld, C. K. Jorgensen (Eds.),Springer, Berlin, **1996**,**85**, 99-103.
[4] P. K. Nair, O. Gomezdaza, M. T. S. Nair, *Adv. Mater, Opt. Electron*. **1992**,**1**, 139-145.
[5] P K Nair, M T S Nair, J. Phys. D: *Appl. Phys*. **1990**,**23**, 150-155.
[6] S. B. Pawar, J. S. Shaikh, R. S. Devan, Y. R. Ma. D. Haranath, P. N. Bhosale, P. S. Patil, *Applied Surface Science*. **2011**,**258**, 1869-1875.
[7] T. Saraidarov, R. Reisfeld, A. Sashchiuk, E. Lifshitz, *Physica*.**2007**,**E 37**,173-177.
[8] D. Yu, Y. Wang, Z.Meng, J. Lu, Y,Quian, *J. Mater. Chem*. **2002**,**12**,403-405.
[9] S.-M.Lee, Y.-W.Jun, S.-N. Cho, J.Cheon**,** *J. Am. Chem. Soc*. **2002**,**124**, 11244-11245.
[10] S. Xiong, B. Xi, D.Xu, C. Wang, X.Feng, H. Zhou, Y.Quian, *J. Phys. Chem*. **2007**,**111**, 16761-16767.
[11] S. Thangavel, S. Ganesan, K. Saravanan. *Thin Solid Films*. **2012**, **520**, 5206-5210.
[12] R. GutiérrezPérez, G. Hernández Téllez, U. Peña Rosas, A. Moran Torres, J. Hernández Tecorralco, L. Chaltel Lima, O. Portillo Moreno. *J. Mat.Sc.Eng*. **2013**, **A 3**, 1-13.
[13]M. Chávez Portillo, J. Martínez Juárez, G. Abarca Ávila, M. Zamora Tototzintle, M. Martínez Barragán, J. R. Cerna, M. Lazcano Hernández, S. Rosas Castilla, B. Crespo Sánchez, A. C. Palacios López, O. Portillo Moreno. J. M. Sc. Eng. **2011**,**A 2**, 410-422.
[14] A. J. Bethune, N.A.S Loud. In Standard Aqueous Potential an Temperature Coefficients at 25 °C, C. C. Hampel, Skokie, II. **1969**.
[15] O. Portillo Moreno, G. Abarca Ávila, J. R. Cerna, J. Hernández Tecorralco, M. Chávez Portillo, J. Martínez Juárez, R. Lozada Morales, O. Zelaya Ángel, *J. Mat. Sc. Eng*. **2012**,**A 1**, 692-704.
[16] O. Zelaya Angel, S. A. Tomas, P. Rodriguez, J. G. Mendoza Alvarez, R. Lozada Morales, O. Portillo Moreno, J. Gonzalez Hernandez, *J. Mater Sci.Eng*.**2011**,**1**, 1-7.
[17] S. Kaci, A. Keffous, M. Trari, O. Fellahi, H. Menary, A. Manseri, L. Guerbous.J. *Luminescence*,**2010**,**130**, 1849-1856.
[18] K.R. Joshi, A.Kanjilal, H. K. Shegal, *App. Surf. Sc*.**2004**,**221** 43-47.
[19] R. K. Joshi, A. Kanjilal, H. K.Shegal, *Nanotechnology*. **2003**,**14**, 809-812.
[20] W. P. Lim, H. Y. Low, W. S. *Chin. J. Phys. Chem*.**2004**,**B 108**, 13093-13099.
[21] Y. Wang, A. Suna, W. Mahler, R. Kasowsky, *J. Chem. Phys*. **1987**, **87**, 7315-7321.
[22] A. S. Obaid, M. A. Mahdi, Z. Hassan, M. Bououdina, Mat Sci. Semicond. Processing. **2012**, **15**, 564-571.
[23] M.Gao, Y. Yang, B. Yang, J. Shen, J. Chem. Soc., *Faraday Trans*. **1995**,**91**, 4121-4125.
[24] J.-H.Chen, C.-G.Chao, J.-C.Ou, T.-F. Liu. *Surf. Sc*..**2007**,**601**, 5142-5145.
[25]R.Rossetti, R.Hull, J. M. Gibson, L. E. J. Brush, *Chem. Phys*. **1985**,**83**, 1406-1410.
[26] S. Wang, S. Yang. *Langmuir*. **2000**,**16**, 389-397.
[27] J. Zhang,X. Jiang, *Appl. Phys. Lett*. **2008**,**92**,141108-1-3